

SEISMIC ATTRIBUTES AND AVO FOR RESERVOIR IDENTIFICATION, NAYIL RESERVOIR, SUTTAIB FIELDS, MUGLAD BASIN, SUDAN

Mahmoud Hassan Ahmed*

Petroleum Geoscience Program, Department of Geology, Faculty of Science, Chulalongkorn University, Bangkok 10330, Thailand.

*Corresponding Author email: houtahassan@gmail.com

Abstract

The study area is located in Muglad Basin, Sudan, and is situated in the western trend of Block 4, GNPOC concession area. The target reservoir Nayil_B sand was deposited in the fluvial-floodplain and lacustrine environments, and is characterized by thin sand interbedded with thick shale of Nayil Formation. The conventional seismic data, due to the thickness of the sand, cannot image the reservoir distribution. Uses of AVO/inversion and seismic attributes have improved the mapping of the reservoir in the study area. The workflow began with rock physics feasibility analysis that indicates the P-impedance parameter as a single parameter that cannot identify any sand from shale. Then, by cross-plotting two parameters it helps to separate sand from shale by using VP/VS ratio, Density against P-impedance and sometimes V-clay. Results from the rock physics indicate that both fields (Suttaib, Suttaib South) have different parameters to discriminate the sand from shale for the same reservoir Nayil_B. The best parameter in Suttaib South is VP/VS ratio, whereas in Suttaib Field it is the density. The low frequency model created for the P-impedance, density and VP/VS ratio, and then the simultaneous inversion was executed to compute the same parameters. Two types of seismic attributes were generated for volume and surface attributes. The attributes show good results for structural features and support the inversion results. The current study concludes that the simultaneous inversion and seismic attributes can image the sand distribution of the Nayil_B reservoir. The results explain the reason for the dry wells that were drilled only based on structural trap not based on sand distribution as shown by the simultaneous inversion and seismic attributes.

Keywords: Suttaib Field, Nayil reservoir, AVO, Seismic attributes, Reservoir Identification

1. Introduction

Muglad Basin in Sudan is one of the largest rift basins created from the Central African Shear Zone (CASZ) (Figure 1). The basin has a general trend of Northwest to Southeast. Exploration activities have proven the petroleum system in the Tertiary and Cretaceous reservoirs. The main reservoir in the study area is thin Nayil sands (Figure 2) deposited during the Tertiary period. It was formed in a lacustrine environment with mainly shale deposition. Oil tested at a deeper depth at Aradeiba Sand (Cretaceous Formation), but, the field is producing only from Nayil sand, and one well from top of Amal Formation (SUS-3). The wells drilled on structural traps and on geological correlations have different sand distributions and fluid contacts. Suttaib fields consist of two structures; Suttaib Main and Suttaib South fields (Figure 2 show the new interpretation horizon of Nayil_B reservoir). Both fields occur in a horst structure.

The normal faults that formed the horst structure have a vertical throw around 100m at both sides and are steeply dipping away from each other and formed graben structure at the deeper area. The study area is highly faulted where the reservoir has been compartmentalized into small blocks ranging in size from few meters to 600m wide.

Seismic attributes and seismic inversion techniques have been applied in Suttaib Fields to discriminate the thin sand layers from the shale. This report will show that sweetness attributes and Simultaneous Inversion show better identification for Nayil sands distribution.

The workflow is listed below;

1. Run volume and surface attributes to find the structural features (Faults) as well as geometrical bodies
2. Apply rock physics analysis to determine the relationship between the lithology and fluid properties and the rock physics parameters.

3. Apply AVO analysis to determine the different classes of the sand reservoirs.
4. Conduct seismic inversion to image the sand distribution.
5. Combine the results together for detailed mapping of the Nayil reservoir.

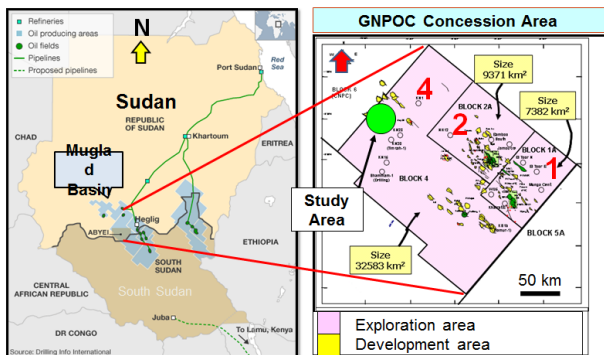


Figure 1. Location map of the study area

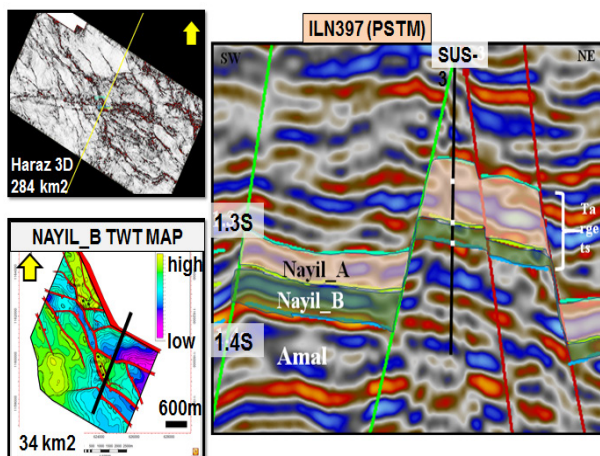


Figure 2. Seismic cross-section along the well SUS-3 showing Nayil sand reservoirs.

2. Methodology

2.1 Rock Physics Analysis

The main objective of the rock physics analysis is to identify the elastic impedance (EI) parameters that can help to discriminate the lithology and hydrocarbons. Cross-plots and histograms were constructed using different parameters for reservoir intervals to find the proper parameters that can predict the rock properties. The EI-parameters were extracted from 6 wells. The cross-plots in Hampson Russell software were applied for P-wave, S-wave, Density, P-impedance, S-impedance, Lambda-Rho and Mu-Rho with respect to water saturation

and V-Clay as a color coded were used to determine the physical parameters that may distinguish sand from shale, and oil sand from wet sands. Moreover, as the depth has a compaction effect on the rock properties, cross-plots were generated to find the effects within the target reservoirs. The lithological and hydrocarbon saturation cut-offs that were applied were based on the company petrophysical values that were derived from reservoir economic studies. The water saturation cut-off used 75%, and 50% for V-Clay cut-off that can separate sand from shale. Using the above cut-off formed an equation in FunctionMod module in Jason software that helped to create the Lithology Log that can distinguish the lithology in cross-plots and histograms.

Lithology log equation as below;

Lithology log = Vclay < 0.5 and Porosity > 0.12 ? 1:0

2.2 AVO and Inversion

Well to seismic ties were applied for 5 wells for the inversion workflow purposes. First, the wavelet was estimated using the PSTM seismic data (Amplitude spectrum). Secondly, wavelet was extracted along wells from the three angle stacks volumes. Finally, the wavelet averaging technique was run to estimate the final average wavelets.

The first step of designing an inversion model is to create a structural model or Solid model. This model incorporated three time horizons (Nayil_A, Nayil_B and Amal horizons), and 5 wells (SU-1, SU-3, SUS-1, SUS-3 and SUS-4). The Solid model designing parameters were;

- Proportional stratigraphy for the upper layer and to follow the base stratigraphy for the lower layer.
- Used Local distance weighted.
- Micro-layer thickness 2ms.

The Solid model was populated with the modeled P-impedance, density and VP/VS ratio. Then use the solid model to construct the Earth model along with the low frequency model of 8Hz. The low frequency model was derived

from wells and used as a trend for the inversion, and to fill the lack of frequency from 0 – 8Hz in the seismic data. Three angle stack volumes (Near, Mid and Far) along with the estimated averaging wavelets were used to transform the P-impedance, VP/VS ratio and density parameters into waveform patterns.

Pre-stack simultaneous inversion was established by using the Constrained Sparse Spike Inversion (CSSI) module of Fugro-Jason software. The results include three inverted models; P-impedance, density and VP/VS ratio.

2.3 Seismic Attributes

Two types of seismic attributes, volume attributes and surface attributes, were generated in the study area. Surface attributes were extracted at the target reservoir Nayil_B. Some attributes were applied to highlight the structural features and other attributes were used to extract the depositional features such as facies and geometry of the sand bodies.

3. Data Set

The data for the study consisted of a 3D seismic volume, well logs, VSP's and stacking velocity.

3.1 Well Data

In addition to the standard LAS files for the log data, petrophysical interpretation for water saturation, porosity and V-clay were also obtained for the study area (Table 1). Well data include well headers, well logs, formation tops and geological cross-sections. Five wells were used in the inversion model (SU-1, SU-3, SUS-1, SUS-3 and SUS-4).

3.2 Seismic Data

Haraz 3D Pre-Stack Time Migration (PSTM) seismic data covered an area of 284 Km², and vertically down to 6000ms. However, the study area was limited to 34 Km²; with approximate range 147 – 283 Inlines and 34 – 314 Xlines. The target reservoirs occur within 1000ms to 1500ms area.intervals. CRP Gathers with Partial stacks volumes were available to perform and maximize the results of the inversion

Log	Wells						
	SU-1	SU-2	SU-3	SUS-1	SUS-2	SUS-3	SUS-4
Caliper	✓	✓	✓	✓	✓	✓	✓
GR	✓	✓	✓	✓	✓	✓	✓
Neutron	✓	✓	✓	✓	✓	✓	✓
Density	✓	✓	✓	✓	✓	✓	✓
Sonic	✓	✓	✓	✓	✓	✓	✓
Shear Sonic	✗	✗	✗	✗	✓	✗	✗
Resistivity	✓	✓	✓	✓	✓	✓	✓
Porosity	✓	✓	✓	✓	✓	✓	✓
V-Clay	✓	✓	✓	✓	✓	✓	✓
Water Saturation	✓	✓	✓	✓	✗	✓	✓
VSP	✓	✗	✗	✓	✗	✗	✗

Table 1. Well log data set for Suttaib wells at the study

study. The partial angle stacks range between; 5 – 17 degrees, 13 – 27 degrees and 21 – 35 degrees. The Bin size is 25x25m (interpolated volume) whereas the original geometry bin size was 50x25m. The results of well ties and wavelets extraction indicated a bandwidth of the seismic wavelet ranging between 6 – 48Hz, with a dominant frequency around 24Hz at the target zone (Figure 3). Using the compressional formation velocity 3100 m/s, the vertical seismic resolution at the target reservoirs is around 32m.

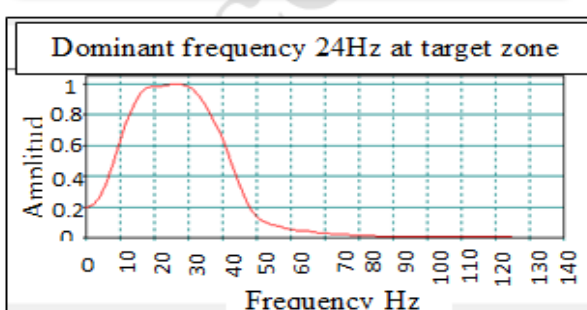
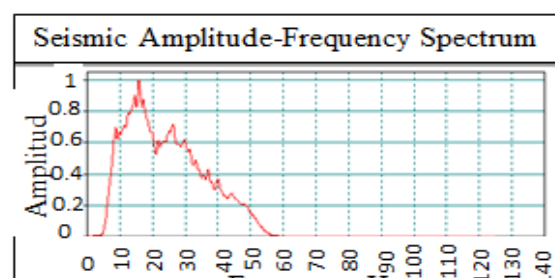


Figure 3. Amplitude spectrums show the dominant Frequencies for the seismic and target zone.

4. Geology

4.1 Tectonic and Structure

The Muglad Basin is the largest graben structure through Sudan and South Sudan Republics. It has three rifting phases during the early Cretaceous to the end of Oligocene (Browne and Fairhead, 1983; Schull, 1988; Fairhead et al. 2013). The study area is covered by Haraz 3D seismic data. A Variance Cube generated from the Haraz 3D seismic data was used to identify the structural trends. A time slice at 1296ms along the Variance Cube clearly identifies the general faults trends (Fault 4). An older fault sets with a NW-SE direction have been cut by younger fault with a WNW-ESE direction forming the observed X-shape structure. The older faults followed the same trend of the Muglad Basin. The X-shape type of faults provided many multi fault-related closures in a Horst style which entrapped secondary migrated oil at Tertiary layers (Nayil sandstone) at Suttaib fields and the nearby fields.

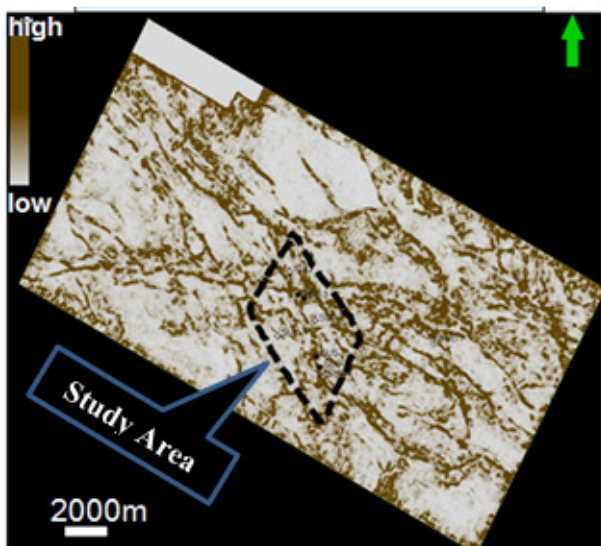


Figure 4. Variance cube attribute, time slice at 1296ms (PSTM volume).

4.2 Stratigraphy

The stratigraphic section of the Muglad Basin occurs due to the high rates of sediments influx into the basin during times of cyclically variable rate and patterns of subsidence. The change in lithofacies primarily reflects variations in subsidence rates of the sub-basins (McHargue et al., 1992).

The Muglad Basin is characterized by the following stratigraphic units:

1. The Precambrian Basement Complex.
2. First rift episode (Early Cretaceous - Albian).
3. Second rift episode (Turonian-Late Senonian)
4. Third rift episode (Late Eocene – Oligocene)

The target reservoirs (Nayil_A and Nayil_B) are related to the third rifting phase, which was created by the reactivation of extensional tectonism during Late Eocene – Oligocene time (Schull, 1988). The Syn-rift cycle initiated with deposition of claystones of Nayil and Tendi Formations that are interbedded with thin sandstone layers. Both formations belong to the Kordofan Group that was deposited in fluvial-floodplain and lacustrine environments (Sudapet Book, 2015) (Figure 5). Nayil thin sandstones represent the main hydrocarbon reservoirs in the study area. A Total of 7 wells were drilled in the study area. There are 4 producing wells and 3 dry wells (Figure 6).

PERIOD	AGE	FM	Ma	(m)	Lithology	Ref.	Dep. Cyc.	Source	Res.	Seal.
NEOGENE	Pliocene	Adok		750		Diffra-4		Sa		
	Miocene		10							
PALAEOCENE	Oligocene	Tendi		1000-400		May 25-1	III			
				750						
Eocene	NAYIL		2.30	250		Gudaim-1		20-30		
Paleocene	Amal		65.5	100		Balome-1		50	Sa	

Figure 5. Stratigraphy Of The Study Area showing the target reservoir Nayil Fm.

5. Well to Seismic Tie

5.1 Correlation of Log Data to Seismic Data

Firstly, the well to seismic tie began with synthetic seismogram creation by using the statistical wavelet for all wells and using the PSTM seismic 3D. The sonic log was calibrated by using the check-shots time to depth relationship of SU-1 for Suttaib Field, and SUS-1 check-shot for Suttaib South Field. Acoustic Impedance (AI) was calculated from density and sonic. Seismic traces around each

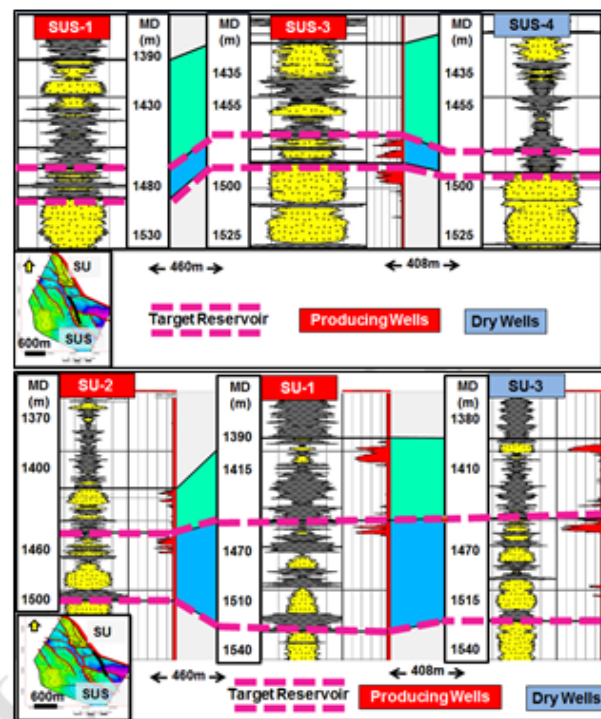


Figure 6. Geological correlation through study area. The red wells are producing wells, where the blue wells are dry wells.

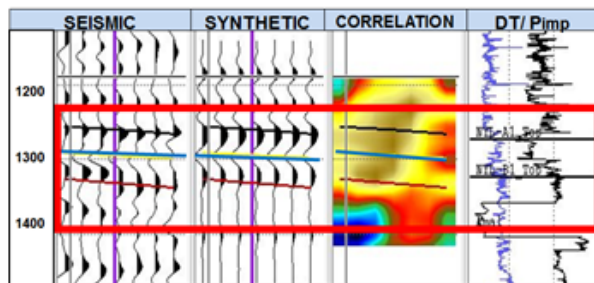


Figure 5. Stratigraphy Of The Study Area showing the target reservoir Nayil Fm.

well used to be compared with the well synthetic traces. Bulk shift, minor stretch and squeeze were applied to match the seismic with well traces. Figure 7 shows an example for the seismic to well tie with correlation up to 0.72. The red box indicates to the target zone.

5.2 Wavelet Estimation

The importance of seismic to well tie is that it will affect the quality of the inversion results. The statistical wavelet (Ricker zero phase – 30Hz) from the synthetic seismogram was used as an input for wavelet extractions for the three angle stacks. Extract amplitude phase spectrum

wavelet for AVO (Near, Mid and Far) was calculated from 5 wells (SU-1, SU-3, SUS-1, SUS-3 and SUS-4). The wavelets for the near angle stacks have frequencies ranging from 25Hz for SU-3, SUS-1 and SUS-4, to 35Hz at SU-1 and 40Hz at SUS-3. The mid angle stack wavelets have frequencies from 25Hz to 45Hz at SUS-3. The wavelets for the Far angle stacks show frequencies from 25Hz to 45Hz at SUS-3. All wavelets have start time -40 to -48, and the wavelength 80 – 100ms. The average wavelets created for each angle stacks (Near, Mid and Far) are shown in (Figure 8).

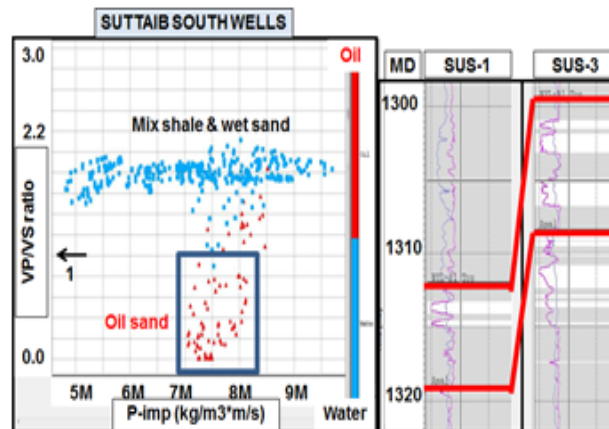


Figure 8. Average wavelets for the near, mid and far angle stack volumes.

6. Interpretation Data

The well tops were provided from the previous geological interpretation. Some corrections for Amal tops after tie-in the wells with the seismic sections has been made to correlate the markers with the seismic reflectors and to match it with the fluid contacts in the depth map. Three horizons and faults were newly interpreted for the project. The new interpreted horizons are: Nayil_A, Nayil_B and Amal horizons (Figure 9).

7. Result and Discussion

7.1 Rock Physics

Rock physics are used to understand the relationship between the geophysical measurements and rock properties. Rock physics parameters were used to distinguish different rock types and fluids. Elastic parameters were used in cross-plots to identify the separation between

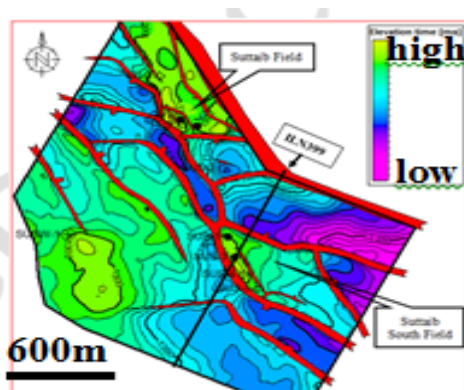


Figure 9. TWT map for Nayil_B target reservoir

oil sand, wet sand and shale. The parameters were; P-velocity, S-Velocity, P-impedance, S-impedance, VP/VS ratio, Poisson's ratio, Lampda-Rho and Mu-Rho. Only one well has Shear log (SUS-2), but, unfortunately it was a dry well that cannot reflect the response of the S-wave through oil sand layers. Estimated S-wave logs were calculated using the Neural Networks in Petrel 2014 software for other wells. The inputs were V-Clay, Porosity, Water Saturation, density and P-wave logs. The validity of the shear logs carried out by cross-plot the P-impedance against the VP/VS ratio parameters with oil/water log as a color code. The polygon for the VP/VS values less than 1.07 was plotted in the well log track and the result was reflected the VP/VS ratio that belongs to the oil sand at the target reservoir. Although the estimated VP/VS ratio has some incorrect input values, however it showed good Lithology discrimination (Figure 10).

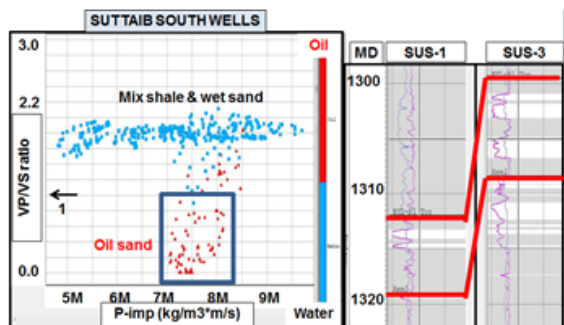


Figure 10. Cross-plot of P-imp against VP/VS ratio with oil/water color code. The white area at the well section reflect the polygon values from the plot (oil sand).

7.1.1 Response of P-impedance and Density

with respect to lithology and fluids

Cross-plots of P-impedance with color codes of depth indicate that P-impedance increases with depth. The depth interval covered the target zone 960 – 1080m TVD. The P-impedance ranges from 1991480 to 10006500 (kg/m³·m/s). Due to small interval of the target zone, the P-impedance does not show a response with depth. The cross-plot of P-impedance against V-Clay, using the Lithology log as color indicator for the target reservoirs interval has an overlap between the sand Impedance and the shale Impedance. It is difficult to determine a cut-off value for P-impedance that related to specific lithology and fluids (Figure 11).

Considering Nayil_B as a separate zone for the cross-plots for Suttaib Field and Suttaib South Field, it showed that, density log can separate sand from shale at Suttaib Field, whereas in Suttaib South Field there is no separation (Figure 12). Density and V-Clay cross-plot at Nayil_B target reservoir showed different situations for both fields. At Suttaib Field the density can separate the sand from the shale at approximately 2.38 g/cc. Shale has higher density than the sand ranging from 2.38 g/cc to 2.72 g/cc, and the sand density ranging from 2.0 to 2.38 g/cc. At Suttaib South Field, the same density value of 2.38 g/cc can separate sand from shale, but a cluster of shale with density points overlapping above the sand makes it difficult to separate all sand from shale in Suttaib South Field using density log parameter.

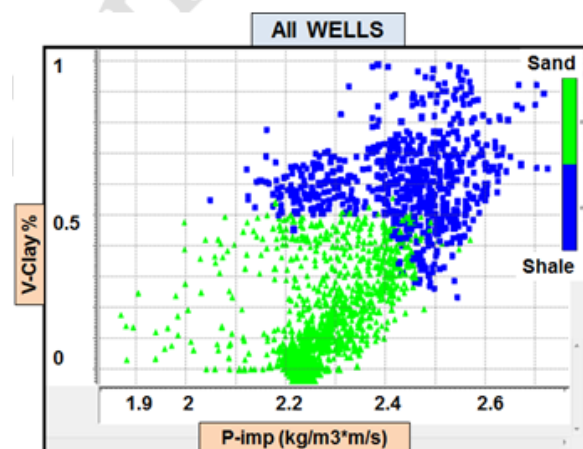


Figure 11. P-impedance cannot discriminate sand from shale in the study area.

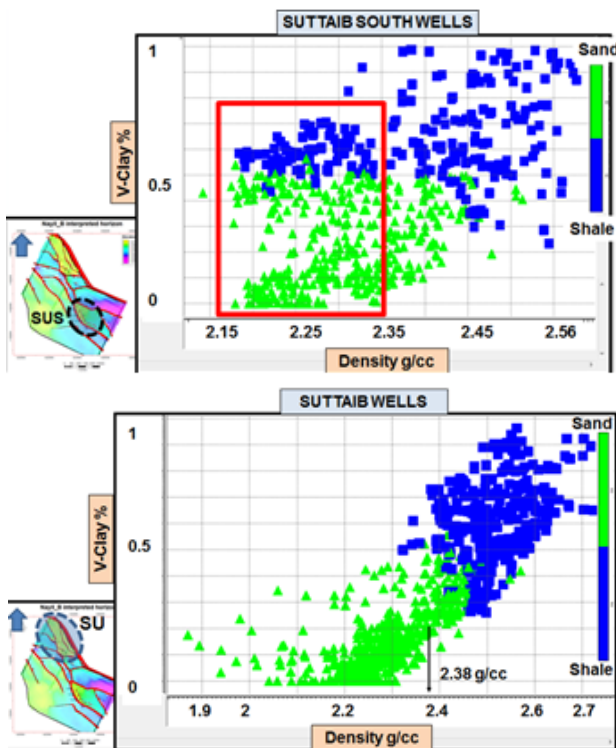


Figure 12. Density cross-plots in Suttaib South Field (upper cross plot) No separation, and Suttaib Field (lower cross plot) can separate sand from shale.

7.1.2 Response of two EI parameters for lithology and fluids discrimination

Using one parameter does not help to separate sand from shale at wells. The second option is to use two different parameters in cross-plots. P-impedance together with estimated VP/VS ratio was applied in this study to discriminate the lithology from the well logs. The cross-plot using the two field data indicate that it is difficult to discriminate all sand from shale. Although a cluster of sand points can be distinguished from the shale, there are still sands that have similar VP/VS ratio values with shale (Figure 13). Similar to the observations with the density parameters, we need to apply cross-plots to each field separately. Suttaib South Field cross plot showed clear discrimination of sand from shale by using VP/VS ratio against P-impedance. The cut-off value for VP/VS ratio is 1.55 for clean sand, above that value there is a mixture of interbedded sand with dominant shale. Suttaib Field cross-plot showed VP/VS ratio value for clean sand around 0.95, however, the

amount of sand points within the shale, which have the same VP/VS ratio values, were high, indicating that we cannot discriminate all sand from shale in this field.

In order to find the fluids response against the rock physics parameters another Oil/Water log has been created that was derived from the water saturation log. Both fields (Suttaib and Suttaib South Fields) have a direct response at the oil zones.

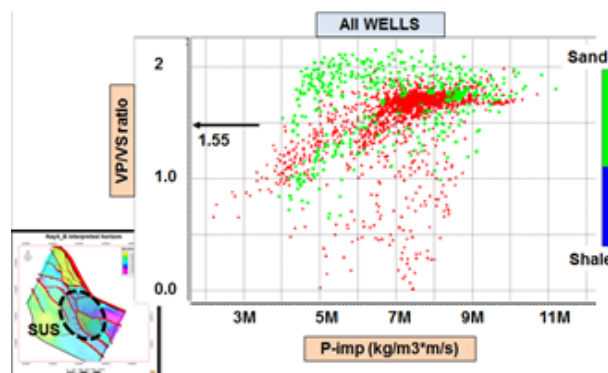


Figure 13. Cross-plot for P-imp and VP/VS ratio for all wells cannot separate lithology.

7.2 AVO Modeling Analysis

Based on the rock physics analysis it was clear that the VP/VS ratio is a sensitive parameter to separate oil sand from wet sand. The oil zone at Nayil_B sand was modeled and identifies good result at one well SUS-3 where at the other wells the results are affected by the quality of the seismic data and wavelet tuning. In well SUS-3, the oil sand characterized by negative amplitude (Trough) at the near angle, and slightly increases towards the far angle stack. This oil sand can be interpreted as Class III (according to Rutherford and Williams, 1998) (Figure 14). There is no obvious distinction between the oil sand and wet sand. The blue curve represents the AVO response measured from the seismic angle stacks, and the red is the response estimated from the well log reflectivity, where the green curve represents the response measured from the synthetic gather. The amplitude character of the seismic and the synthetic can be correlated.

In Suttaib Field, it was difficult to find the AVO response. The reason for that is due to

noise and wavelet tuning. In addition to that, the angle stacks traces were not well aligned perfectly. The angle stacks volumes required reprocessing to flatten the reflectors in a way that the different angle traces will align at the same event.

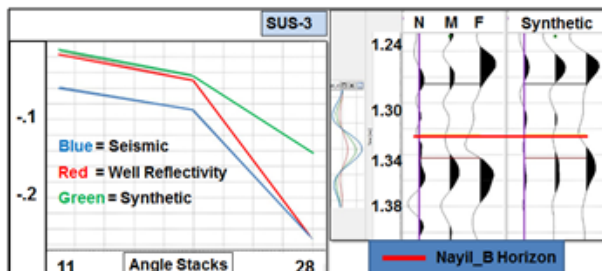


Figure 14. AVO response at SUS-3 well indicating the oil sand in Nayil_B is Class III.

7.3 Simultaneous Inversion – Model Result

Three inversion models were generated from the Constrained Sparse Spike Inversion (CSSI) module of Fugro-Jason software. The resulting models are; P-impedance, density, and VP/VS ratio (Figure 15).

7.4 Simultaneous Inversion – Model QC

Basically the inversion model QC procedures are built-into the RockTrace module. There are QC methods that are automatically generated for each angle stack volumes (Near, Mid, and Far),

- Seismic – Synthetic Correlation

This QC reflects the correlation coefficient between the seismic traces and synthetic traces based on CSSI estimation. For Far angle stacks volume the correlation having an average of 0.95 (prior CSSI 0.12). Whereas the near stack has a correlation coefficient 0.75 (prior CSSI 0.15).

- Average signal to noise ratio Signal to noise ratio for the Far stack around 10 and 12 for the Near stack.

7.5 Blind Test QC

An alternative QC type that can be applied is the Blind test. Two wells were excluded from

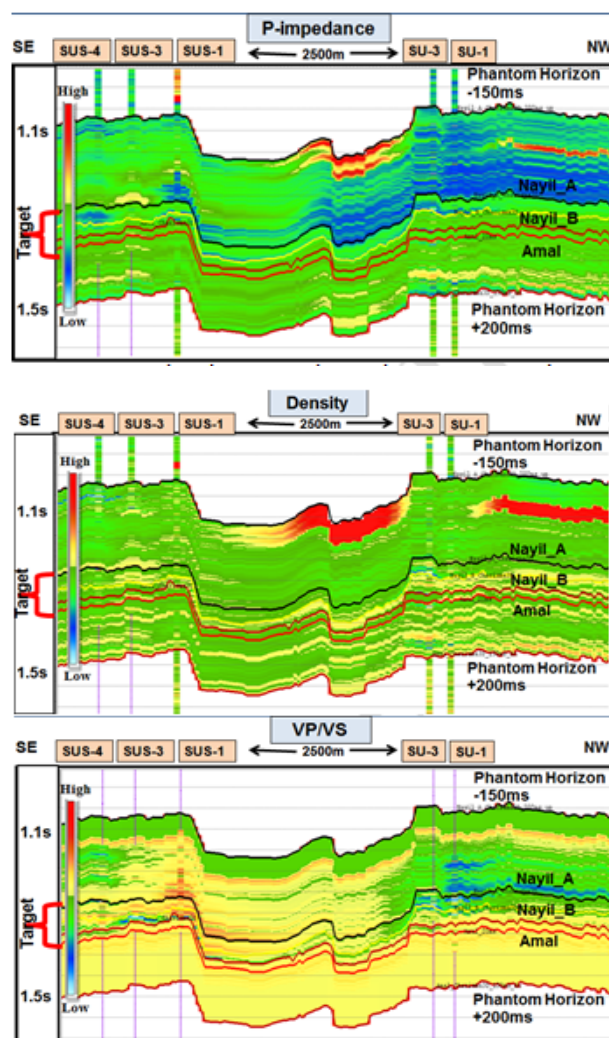


Figure 15. Simultaneous inversion output volumes (Density, VP/VS ratio and P-imp).

the inversion process, SU-2 and SUS-2. For SU-2 according to the geological cross-section, the geologist believes the target zone was faulted out. Whereas in SUS-2 the well was excluded because it was dry well even though it is the only well having shear log. The shear log from SUS-2 well was used as the calibration log for the estimated S-waves from the neural network for the other wells, and to validate the lithology resulted from the CSSI. Figure 16 has SUS-2 as a blind test well displayed on inverted density volume. The comparison of the SUS-2 with Inverted density volume indicates good correlation. The red arrow pointed to the thin sand layer in the well section in the inverted density volume. The red color

in the inverted volume represents sand, the green represents higher density with respect to shale and shaly sand.

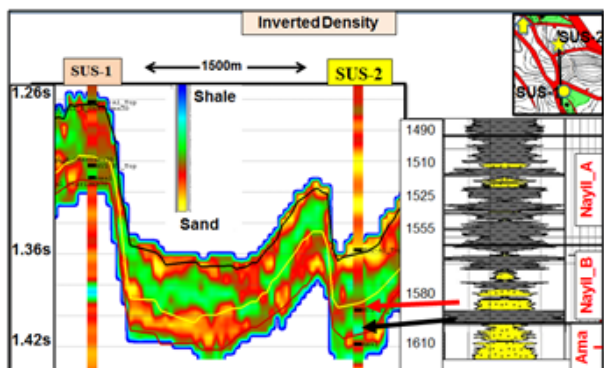


Figure 16. Simultaneous inversion Blind test QC.

7.6 Seismic Attributes

Seismic attributes generated to find the structural features and any geometrical bodies. The best structural attributes were; Variance Cube, Structural Smoothing, Most Positive Curvature and Most Negative Curvature. Furthermore, geometry attributes that helped to characterize the channelized bodies were Sweetness, Root Mean Square (RMS) amplitude, Relative Acoustic Impedance and Iso-frequency (Spectral Decomposition). The channels that could not be observed were probably due to their thinner thickness. The net reservoir thicknesses of Nayil_B layer range from 8 – 12 m at Suttaib South Field and 12 - 22m at Suttaib Field. The seismic tuning thickness is around 32m. All the above mentioned attributes were generated in PSTM and angle stacks seismic volumes.

Most Positive Curvature attribute reflect the highly faulted feature of the field (time slice at 1296ms) (Figure 17). The Red circle at Suttaib Field focuses on the fractures that affect the horizon interpretation and the fault picking, and influence directly on the wavelet estimation from the wells. The faults trends, showed by the black arrow, have the NW-SE direction related to the old faults those occurred parallel to the Muglad Basin trend. The red arrow is related to the new faults trends.

Sweetness attribute in general helps to identify sand shale distribution in siliciclastic

environment. In the generated time slice (1304ms), the Sweetness attribute from the Near angle stack (5 – 17) at Nayil_B layer shows different lithological bodies distributed through the slice. Calibrating the bodies with the wells confirms that the high sweetness amplitudes represent sand (yellow color), where the lower values relate to shale or non-reservoir bodies (black color) (Figure 18). The red polygons represent Nayil_B sand bodies in the time window 1292 – 1312ms at Suttaib Fields.

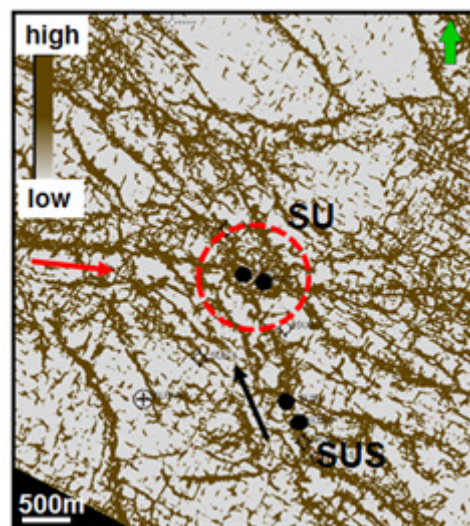


Figure 17. Most positive curvature

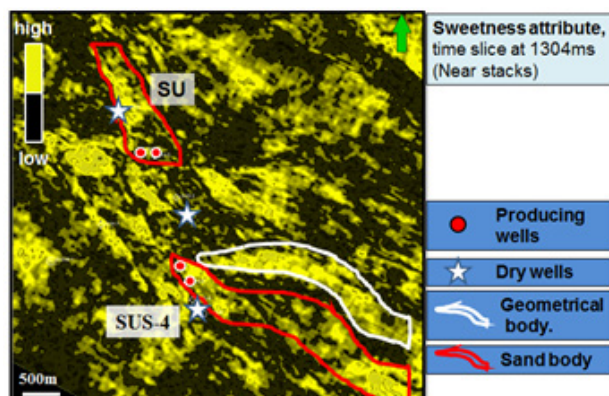


Figure 18. Sweetness attribute time slice at the Nayil_B reservoir. The red polygon represents sand body at the target reservoir, and the white polygon represents a geometrical body at the downthrown side of the fault (younger formation).

8. Interpretation of Lithology and Fluid Distributions

Stratigraphic volume for VP/VS ratio

volume has been created in a 3D volume and displayed in a map view showing the top sand distribution of the target reservoir (Figure 19).

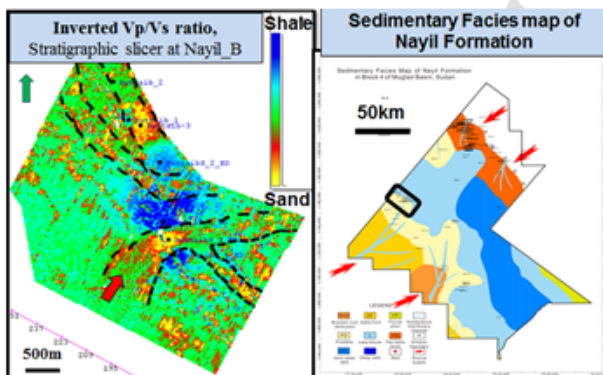


Figure 19. Inverted VP/VS showing channelized features that similar to the facies map generated by research institute for GNPOC. The red arrow represents the direction of the distributary channels.

Furthermore, the result of the CSSI inversion was used as an input for the Facies and Fluid Probabilities (FFP) module to generate different volumes of lithology probabilities, by using the relationship between the Elastic parameters through the cross-plots and the sand-shale log as a color code (Figure 20).

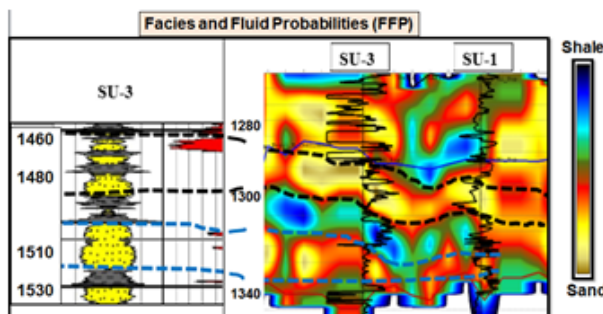


Figure 20. The most probable FFP model result correlated with SU-3 well. As the color code indicates blue and green for shale, yellow and red for sand, it is correlatable with the well

The Sweetness attributes at the top of Nayil_B layer, shows geometrical sand bodies that are confirmed with the well drilling data. The depth map when overlaid above the Sweetness attribute explains the reason for the dry wells. The wells were drilled away from the sand bodies

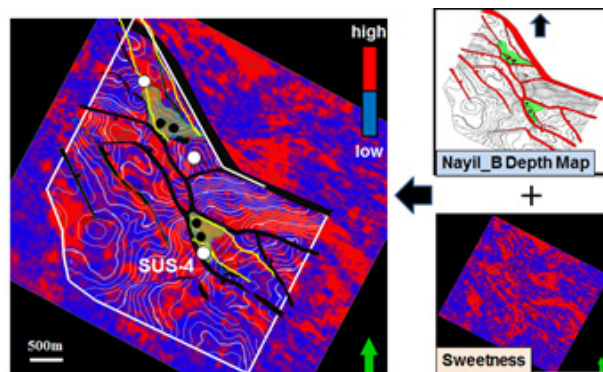


Figure 21. Nayil_B depth structure map merged with the Sweetness attribute result.

9. Conclusion and Recommendations

- Acoustic Impedance cannot discriminate sand from shale.
- It is important at the study area to separate the reservoir into two fields while looking for the parameters cut-off values.
- Although the estimated VP/VS ratio has some incorrect input values, however it showed good Lithology when applied with P-impedance and V-clay in cross-plots or in a Histogram especially for Suttaib South Field.
- Density log showed better separation specifically at Suttaib Field.
- The Low frequency model generated as a simple model, it is highly recommended to create a complete static model as an input data for the CSSI inversion.
- Seismic attributes helps in recognizing structural features such as Variance Cube and Most Positive/Negative Curvatures. Sweetness as well as the RMS amplitude have good results in identifying the geometrical bodies.
- The seismic data is still showing high noise that affected the wavelets estimation.
- More angle stack volumes to obtain better results from the inverted density.

10. Acknowledgements

I would like to express my deep appreciation to Petroleum Geoscience Program, Chulalongkorn University, and

and Prof. Joseph Lambiase (Program Manager) for giving me this chance for Post-graduate study. My profound gratitude's goes to Chevron Company for providing scholarship fund, which allowed me to undertake this Master degree.

I would also like to give my sincere gratitude to Mr. Angus Ferguson for his useful guidance, valuable feedback and constant encouragement he provided throughout the duration of the study time. Working under his supervision was an extremely knowledgeable experience for me.

My great appreciation goes to all the instructors in the program for their contribution, valuable information's and experience they share with students.

I would to take this opportunity to thank my company Greater Nile Petroleum Operating Company (GNPOC) for giving me the data that I used for the project.

My grateful thanks are also extended to my colleague Mr. Mohamed Elnoor for his assistance and support in using Fugro-Jason Software throughout the project.

I must express my gratitude to my Family and my wife, Ranya Elmahi, for her continued support and encouragement.

Special thanks to Chula staffs. Finally, I would like to thank all my friends and colleagues in the program for their help and support and the great study atmosphere that we had during our study and field trips.

11. References

Browne and Fairhead, 1983. Gravity study of The Central African Rift System: A model for Continental disruption, 1. The Ngaoundere and Abu-Gabra Rifts, Tectonophysics, v. 94, p. 187-203.

McHargue et al., 1992. Tectono-stratigraphic Development of the interior Sudan rifts, Central Africa, Tectonophysics, v. 2013, p. 187-202

Personal Communication, GNPOC Company, By CNPOC International Center, 2015.
Rutherford, S. R., and Williams, R. H., 1989, Amplitude-versus-offset variations in gas sands: Geophysics, 54, 680-688.

Schull, 1988. Rift Basins of interior Sudan: Petroleum exploration and discovery, AAPG Bull, v. 72, p. 1128-1148.

Sudapet Book, 2015. Petroleum Geology and Resources of the Sudan, p. 131-132.